Sensitivity Improvements for Space Domain Awareness using Satellite Tracking on a Nanosatellite

Alexander J. Pertica,
Terran Orbital Corporation

Willem de Vries
Physics Division,
Lawrence Livermore National Laboratory

Chris Shaffer, Jeremiah DiMatteo, Robert Goodloe
Emily Milne, Bailey Cortright, Weston Pruitt, Kyle Clarke
Brian Fox, Christian Fuller, Michael Higgins
Terran Orbital Corporation

Abstract Summary

We present the results from a flight campaign dedicated to exploring the utility of satellite tracking mode for Space Domain Awareness (SDA) metric observations from a nanosatellite in LEO. Metric observations from space-based assets are typically obtained in inertial pointing mode. In this mode, stars are fixed and satellites streak through the frame. Streak length depends on the target satellite's crossing velocity. There are two significant limitations to operating in this mode that apply mainly to LEO-to-LEO observation. The first limitation is sensitivity, which is limited by the time it takes for the target satellite to cross a pixel on the sensor's focal plane array. Increasing sensor exposure duration beyond the pixel-crossing time does not improve the signal per pixel – it only lengthens the satellite streak. Streak length is the other significant limitation in LEO-to-LEO metric observations. To obtain a useful metric observation, the streak endpoints must lie within the frame. For targets with large crossing velocities, it is necessary to decrease exposure to limit streak length. This can result in not detecting sufficient stars in the scene to obtain a good astrometric solution for the frame-center coordinates.

In this effort, we explore using satellite tracking mode for SDA. In this mode, the target satellite is fixed in the frame, but the background stars are streaking as shown in Fig. 1. Although exposure can be increased in this mode to improve the signal-to-noise ratio on dim targets, there is a limit imposed on metric observations by the requirement to obtain good astrometric solutions on streaking stars in the background. However, there is still potential utility for images where an astrometric solution is not possible (e.g., . detecting a dim object in rendezvous proximity orbit to a bright object).

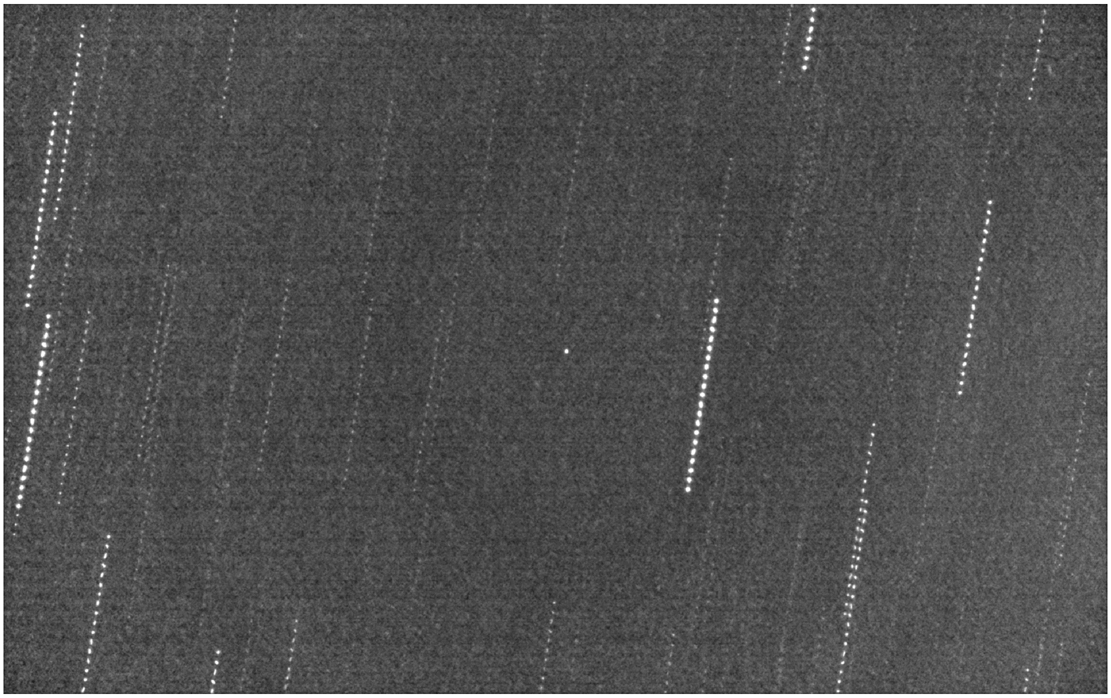

Fig. 1. GEO satellite RSO-tracking image (composite of 21 images on 2s centers) collected with the GEOStare2 CubeSat. The target satellite is the dot in the image center. The strings of dots are stars streaking across the sky.

For this study, we upgraded the GEOStare2 6U imaging nanosatellite with a satellite tracking capability. GEOStare2 launched in May 2021 and features dual 8.5cm aperture panchromatic imagers, one of which was optimized for SDA applications. Prior to the upgrade, GEOStare2 demonstrated the capability to provide inertial pointing mode metric observation on objects in GEO, MEO, and LEO. It has returned over 50,000 observations since launch. Since the satellite was already equipped with a rate mode capability, the upgrade added the ability to propagate ECI State Vectors using the onboard flight computer to generate pointing quaternions for target satellites.

We present the results from a dedicated flight campaign using GEOStare2 to explore satellite tracking mode for SDA applications across the GEO, MEO, and LEO orbital domains. This study explores sensitivity improvements obtained by increasing exposure and the practical limitations on obtaining good astrometric solutions in this mode. In addition, we discuss attitude determination and control system (ADCS) estimation and pointing performance impacts on imaging sensitivity. We also look at limitations imposed by the satellite's maximum slew rate on targeting opportunities in LEO and compare this to inertial mode limitations imposed by streak length. Figure 1 above shows a composite image created from a typical RSO tracking mode image collection dataset, illustrating a fixed satellite and multiple stars streaking across the frame.

Implementation

Resident space object (RSO) tracking was implemented on the GEOStare2 6U CubeSat. GEOStare2 is a multi-mission optical satellite developed jointly between Terran Orbital and Lawrence Livermore National Laboratory as a pathfinder for demonstrating advanced Earth observation (EO) and Space Domain Awareness (SDA) techniques from an agile boresight nanosatellite. It launched in May 2021, into a 53° inclined orbit at 575 Km altitude. The satellite is equipped with reaction wheels and torque rods for attitude control and is capable of slew rates in excess of 3° per second. The satellite design minimizes boresight drift by using short solar panels with rigid latches. In inertial pointing mode, we typically observe boresight drift of less than 6 arcseconds per second.

Figure 2. GEOStare2 prior to launch

The optical payload for GEOStare2 was developed by Lawrence Livermore National Laboratory (LLNL). The payload leverages the monolithic telescope technology for making robust and compact telescopes from a single block of high-purity fused silica. Monolithic telescopes are highly compact and robust to withstand challenging thermal and vibrational environments. LLNL and Terran Orbital have jointly demonstrated the suitability of this technology for on-orbit use and over a dozen monolithic telescope-based imagers have been launched to date.

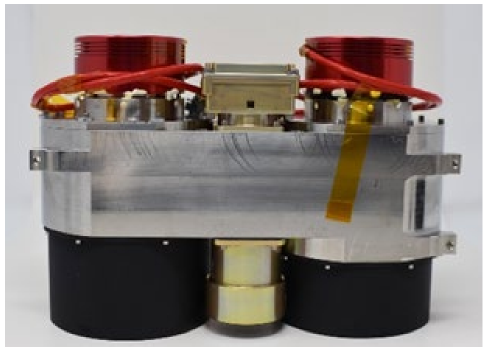

Fig. 3. Lawrence Livermore National Laboratory imaging payload for GEOStare2

The GEOStare2 optical imaging payload consists of two side-by-side co-boresighted imaging channels. Both channels feature an 85 mm aperture monolithic telescope coupled to a complementary metal-oxide semiconductor (CMOS) focal plane array. Channel 0, the Narrow imager, has a 650 mm focal length and an RGB focal plane array (FPA) and is used exclusively for EO. This work employed channel 1, the Wide imager, exclusively since it was specifically optimized for SDA featuring a shorter 306 mm focal length and a panchromatic FPA. Properties for both imagers are presented below in Table 1.

Table 1. GEOStare2 payload properties

Payload Properties	Wide Imager	Narrow Imager
Boresight body axis	Z	Z
Telescope	V3’	V4
Clear Aperture (cm)	8.5	8.5
Focal Length (m)	0.31	0.65
Pixel Pitch (micron)	5.9	2.4
X pixels	1,936	3,096
Y pixels	1,216	2,080
Max bits	12 bits	14 bits
GSD (m) @ 575 Km	10.9	2.1
Platescale (‘/pixel_	3.92	0.77
X Ground Extent (km)	18.5	5.8
Y Ground Extent (km)	11.6	3.9

Since launch, we have employed the Wide imager on GEOStare2 to obtain metric observation of RSOs in GEO, MEO, and LEO with the satellite in inertial pointing mode. For inertial pointing, the satellite attitude control system attempts to keep the boresight pointed to a fixed celestial coordinate (right ascension and declination) using star tracker updates to the gyro-based inertial measurement unit (IMU). In planning collects, we use publicly available catalog two-line element sets (TLEs) to predict when the satellite has clear line-of-sight access to target RSOs under favorable illumination conditions. Commands are then uploaded to the satellite to slew to the celestial coordinate in advance of the collection opportunity and we allow for a brief settling period prior to capturing a series of images as the RSO crosses the FPA's field of view. To date, GEOStare2 has collected over 50,000 metric observations in this manner.

A rate mode capability has existed on GEOStare2 since launch for Earth orbit (EO). To implement RSO tracking capability, new flight software was developed and uploaded to the vehicle in July 2023.

Resident Space Object (RSO) tracking is a well-defined problem in theory but difficult to execute in practice. The guidance algorithm used to track an RSO has several required inputs: the observing spacecraft's inertial attitude, the orbital estimate of the observing spacecraft, and the orbital estimate of the RSO. With these inputs, it is straightforward to construct the relative line-of-sight (LOS) pointing vector with which to align the optical imager. However, many challenges arise when implementing and executing this onboard a spacecraft with the intent to image targets in LEO, MEO and GEO. Examining sources of these guidance algorithm inputs gives insight into the impacts of estimation and pointing performance on RSO imaging.

The foundation of RSO tracking lies in accurate orbit determination (OD). This involves estimating the precise orbital parameters of both the observing spacecraft and the target RSO. GEOStare2 is equipped with a GPS and an Extended Kalman Filter (EKF) for orbital state estimation for which the dynamics model includes the Earth Gravitational Model EGM2008, solar and lunar gravity perturbations, and aerodynamic drag. This high-fidelity orbit dynamics model ensures the EKF has accurate propagation during time steps without measurement updates from the spacecraft's GPS. In relation to RSO tracking, it is paramount to have accurate and smooth spacecraft position estimates. When constructing a vector with its tail at the spacecraft position and the head at the RSO position, inaccurate observer estimates result in biases that can move the target from the center of the image or off the image altogether. A noisy observer estimate results in the target exhibiting oscillatory or jittery movement across multiple images.

The RSO orbit estimation likewise contributes to imaging sensitivity, however it poses its own difficulties. The direct re-use of existing OD EKF architecture for RSO orbit estimation is not possible. The EKF, as a recursive filter, relies on sequential measurement updates. GEOStare2 is not currently equipped with a sensor that can provide orbital state measurements for other objects. This lack necessitated a redesign for an RSO propagation architecture. Fortunately, the underlying high-fidelity orbit dynamics model within the OD EKF could be leveraged in the RSO implementation. This lent itself to a modular and reusable design pattern. The versatility of the orbit dynamics model proved particularly beneficial for the RSO propagator since different orbital regimes demand distinct modeling considerations. While drag is a dominating force for LEO targets, it diminishes greatly for objects in MEO and GEO. Conversely, solar and lunar gravity perturbations, often negligible in LEO, become critical for MEO and GEO. By dynamically configuring the modeling of these perturbations, we can optimize for both fidelity and computational load specific to each orbital regime. The primary distinction between the RSO propagation and the spacecraft's own OD EKF lies in the update frequency. The spacecraft's OD EKF benefits from real-time GPS measurements at 1Hz, offering frequent updates to correct for propagation error. Conversely, the RSO propagator relies on an initial seeding of information provided by a ground operator before each imaging session. This one-time state seeding introduces a major disadvantage. Uncertainties in the RSO's initial conditions— position, velocity, and epoch—can significantly skew propagation outcomes. Furthermore, small errors in these initial parameters are compounded by the error accumulation inherent in numerical methods and unmodeled or poorly modeled perturbations. To minimize this error, the RSO states are propagated on the ground using an in-house high-fidelity propagator before uploading to the vehicle's onboard RSO propagator to seed the spacecraft with the most accurate RSO state possible.

Another significant source of error in RSO imaging stems from attitude determination (AD) algorithms. When the attitude estimate is inaccurate, it can result in substantial tracking error, particularly with distant targets. Such inaccuracies might cause targets to appear off-center or even fall entirely outside the optical imager's field of view. Additionally, a noisy attitude estimate can cause an imaged target to bounce around between multiple captures, or within a long exposure capture. This decreases signal-to-noise ratio and can introduce blurring. When imaging moving targets, the vehicle may need to track at high rates. Under these conditions, star trackers deliver less frequent and noisier measurements. Gyro misalignment and scale factor errors become more pronounced, thus degrading attitude estimation.

GEOStare2's ADCS software employs a 21-state EKF, fusing measurements from star trackers, gyros, magnetometers, and sun sensors. While this setup adequately supports mission operations like ground imaging, the heightened sensitivity required for RSO imaging necessitated additional calibration. Calibration first involved precisely aligning a designated primary star tracker with the optical payload boresight, ensuring that the ADCS attitude estimate would accurately center an RSO target in the optical imager's field of view. Subsequently, the other star trackers were synchronized with this primary tracker to minimize discrepancies in the attitude quaternion measurements. This minimized high frequency attitude estimation noise from sensor misalignment, reducing it to the low frequency effects of thermal drift. The final calibration step is with the gyro adjustments: aligning them with the primary star tracker, estimating skewness, and calculating scale factor error. Corrections based on these estimations are then integrated into sensor processing to minimize measurement noise. This greatly improved GeoStare2's AD knowledge and stability.

The final component of any ADCS is its control law design. For RSO imaging, our system employed the spacecraft's default controller architecture, with a few distinct modifications. Notably, the controller bandwidth was increased. By adopting a less conservative controller gain set, we achieved greater bandwidth, albeit at the cost of reduced relative stability margin. Still, these adjustments were kept within the designed bounds of 6dB and 30 degrees for gain margin and phase margin, respectively. Given that RSO imaging sessions are typically brief, it is reasonable to assume that momentum accumulation will not be significant throughout. This assumption enabled us to deactivate the torque rod control, thereby eliminating an external disturbance. Lastly, reaction wheels realize a larger range of speeds when torquing the spacecraft to track dynamic targets. This can increase the frequency of zero crossings which induce mechanical vibrations on the system. Momentum biasing the reaction wheels such that their mean speed is higher minimizes this disturbance.

In essence, while the theory of RSO tracking seems direct, real-world scenarios present numerous challenges. Each step, from orbit determination to control design, demands precision to ensure the target is accurately captured. GEOStare2's ADCS addressed each complication and successfully estimated, tracked, and imaged RSOs in LEO, MEO, and GEO.

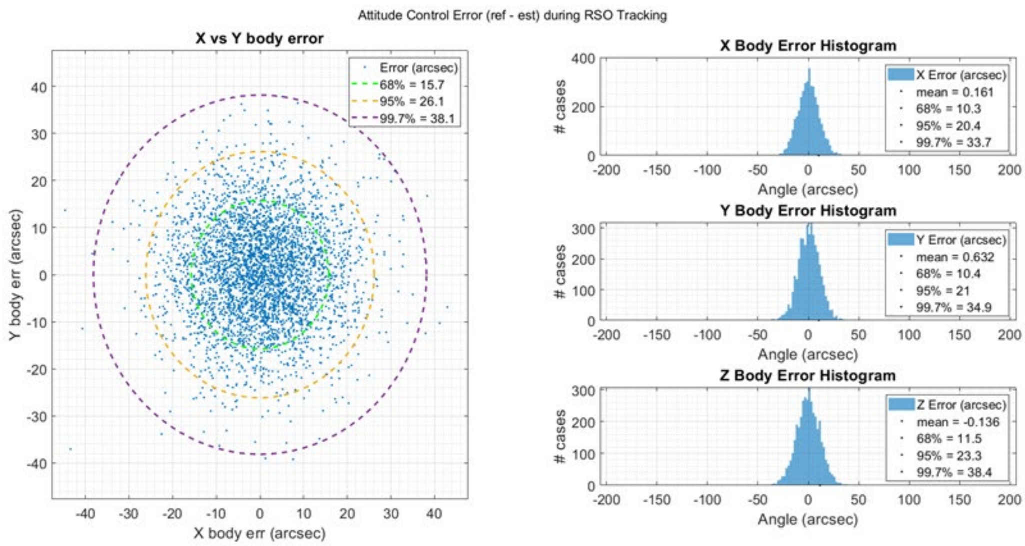

Figure 4. Illustrating the pointing performance for GEOStare2 while RSO tracking. The scatter plot on the left depicts the spacecraft's control error across the boresight. The three histograms on the right show the control error distributions for each individual axis

GEOStare2 takes images by passing time, location, and camera parameters into onboard schedule management scripts that allow operators to use guidance, navigation, and control code to design and schedule RSO tracking imaging sessions. The spacecraft is prompted to enter an initialization state and begin propagating the RSO seed. After being allowed to propagate for several minutes while the vehicle slews to the desired position, an image session will begin, using this propagation to track the object for the duration of the capture time.

Rationale for RSO tracking

A limitation of inertial tracking mode is that RSO observation is limited to the time in which it crosses the field of view (FOV). This can be mitigated, to an extent, by making the FOV larger. However, this comes at a cost of diminishing metric precision as the platescale increases with the FOV. For LEO-to-GEO collects, the FOV crossing limitation is not severe because GEO RSOs present low crossing velocities. For LEO-to-LEO collects, crossing velocities are typically in the range of 300 to 3,000 arcseconds per second. Therefore, possible observations time windows are at best tens of seconds and more typically just a few seconds. With RSO tracking, observation time windows are limited only by line of sight and illumination conditions. Advantages of extended observation time windows are twofold: facilitating continuous monitoring/tracking, and increased sensitivity/detectivity. There are, however, challenges to using RSO tracking mode to obtain metric observations. The primary challenge comes from the fact that stars are now streaking through the FOV, potentially overlapping with the target object, and creating complications for determining boresight coordinates using stellar astrometry. We modified our approach to processing GEOStare2 images as a result.

Image processing approach

The images, as they come off the GEOStare2 spacecraft, are unprocessed lossless compressed TIFF files. Before the series of images are combined, either as an average or a median frame, each individual image is corrected by a master dark frame to remove warm pixels, as well as a geometric correction to remove the small pin-cushion distortion inherent in the GEOStare2 imaging telescope. Small spacecraft boresight wander has been taken out by aligning the frames according to the target frame position as predicted by the orbital elements of both the GEOStare2 satellite itself and the target orbit. In general, we found this process very accurate, and we did not need to resort to aligning based on fitted target positions. The latter approach would not work on targets as faint as object A, D, or E in Fig. 4.

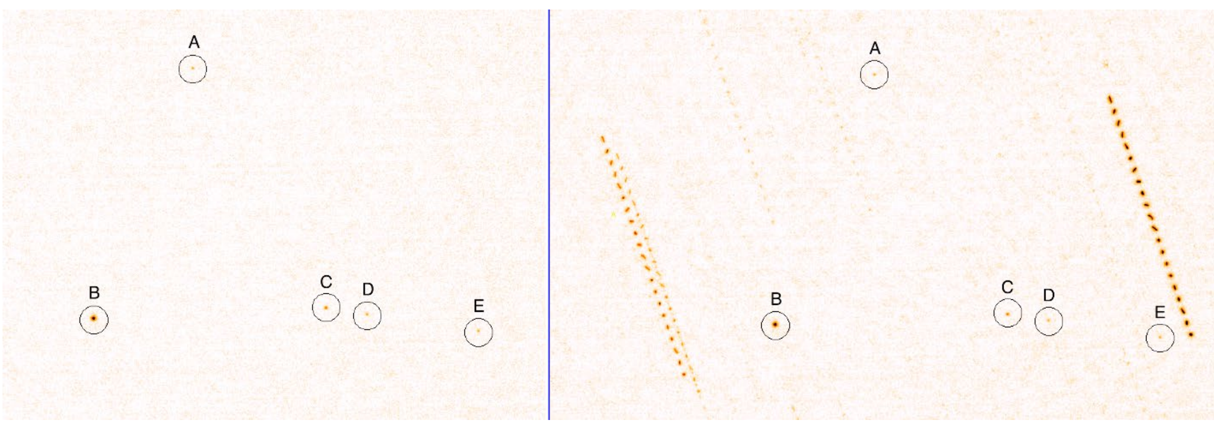

Figure 5. Median combined image (left panel) of a series of 21 individual frames, compared to the average mean (right panel). Since the stars move and the targets do not with RSO tracking, the median frame makes targets stand out by effectively removing the streaking stars. This particular collection example captured multiple Geo-stationary satellites across a series of exposures. Five satellites have been labelled in this zoomed-in image frame. The streaks in the right panel are stars that move through the field of view as the spacecraft keeps target A near the center of full image.

Regardless of the precise alignment, the frame combination process removes image imperfections and other fixed pixel-to-pixel variations between frames by rejecting outliers. In addition, the median combined frame is rather effective in removing anything that moves across the sensor over the duration of the target collection sequence. Normally, in sidereal / inertial tracking mode, this affects the satellites, but in target tracking mode the satellite(s) are stationary, and the stars streak across the frame.

The results are shown, at least as a zoomed-in part of the larger field of view in Figure 1. For this particular collect on August 21, 2023, we targeted geostationary satellite A, but were able to also capture several nearby satellites (6 in total, of which 4 are shown in Fig. 4). The right panel is the average frame that still includes the stellar streaks, while the left median panel has the stars removed almost completely. The next section focuses on the benefits of this median combined, target-tracked image product.

RSO tracking data collection campaign

In July and August of 2023, we conducted an intense data collection campaign employing GEOStare2 to collect observations in RSO tracking mode. We selected targets in GEO, MEO, and LEO and sought to collect datasets over a range of slew velocities. Most collects utilized an exposure duration of 500ms, and we collected 21 frames on 2s centers.

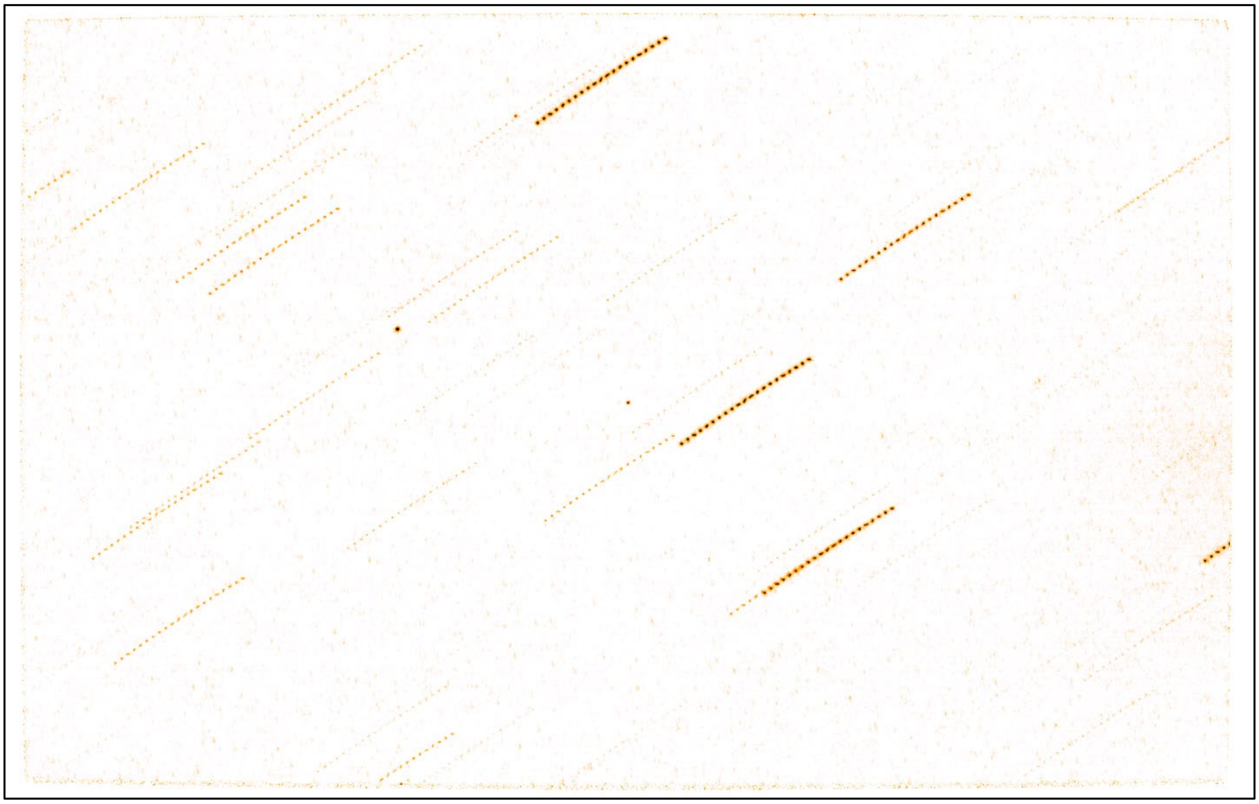

Figure 6. Composite image for a LEO RSO rate mode collect. In addition to the target satellite, several others are relieved in this image

S/N improvements

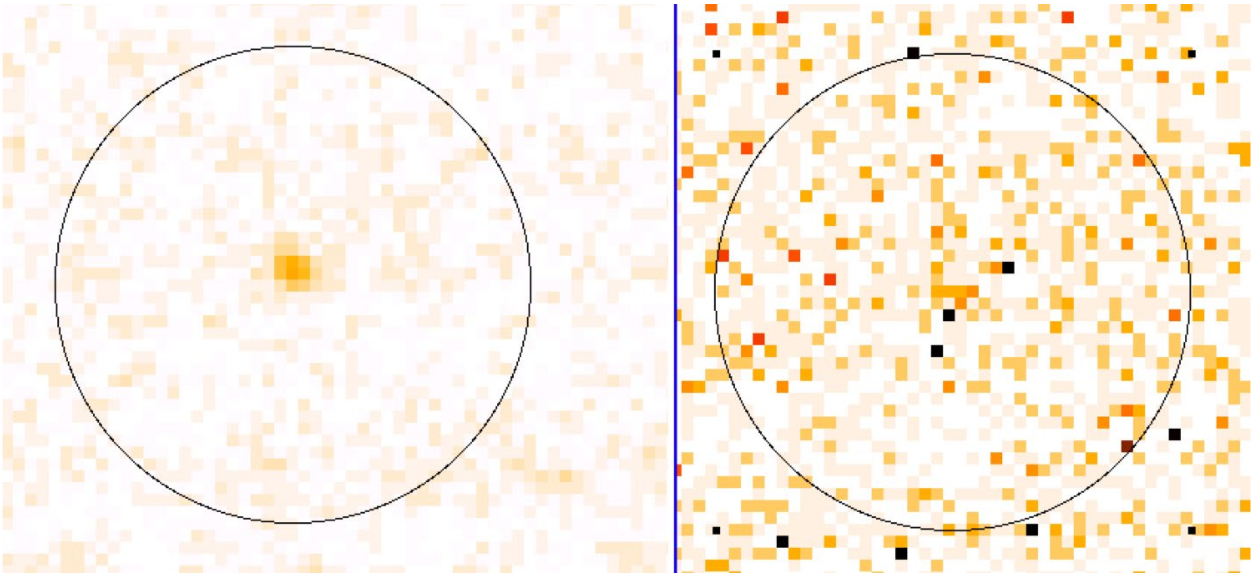

Figure 7. Target A from Fig. 6 zoomed in and compared to a single, noisier frame. The S/N ratio increased dramatically to about 9, up from about 1.5 in the right frame.

Combining frames, as outlined in the previous section, has several inherent advantages. It not only increases the target signal by properly aligning the frames, but it also allows for effective removal of unwanted artifacts and other contamination sources. Even though each subframe comes with its own read-noise contribution compared to a single, equivalently long exposure, the modest read-noise increase (as the square root of the number of subframes) does not limit overall image usefulness as much as the difficulty in artifact removal in a single deep frame.

A sense of this can be gleaned from Fig. 7. The right panel shows target A from Fig. 6, now in a single subframe. Its measured Signal-to-Noise ratio (SNR) is only about 1.5 if one carefully removes the obviously present warm pixels (dark in Fig. 7) from statistical consideration. The focal plane in the GEOstare2 satellite is not thermally controlled, and its operational temperature variations are significant enough (it typically varies between 10 to 25 degrees C) that the master dark frame does not fully remove these warm pixels. This problem becomes more pronounced for longer exposures. The individual frame in Fig. 7 is exposed for 500 ms, which is at the shorter range of our typical exposures. Even here, the faint target A flux is compromised by the presence of warm pixel residuals. One would be hard-pressed to claim a valid signal if not for the positional prior.

The left panel shows the median combined image of 21 x 0.5 = 10.5 second total exposure. The SNR ratio for this now-much-cleaner image has improved to 8.9, a little larger than naively expected by multiplying 1.5 by the square root of 21 (SNR=6.9). This is due to effective pixel artifact suppression.

Image sensitivity

Table 2. List of apparent (unfiltered) magnitudes of labelled satellites in Fig. 1.

Object	Magnitude (unfiltered)	Error in magnitude	Signal-to-Noise Ratio
A	12.42	0.12	8.9
B	9.70	0.013	83.0
C	11.61	0.06	15.5
D	12.24	0.10	10.1
E	12.20	0.09	11.8

We applied aperture photometry methods common in the astronomy community. Frames were photometrically calibrated using all catalog-matched stars in the full frame of view. Based on the correlation between measured count rates and calibrated catalog R-band magnitudes for these matched stars (using the UCAC-4 catalog, see ref [X]), a best fitting relation between measured flux counts and corresponding apparent magnitude can be obtained. This is not a perfect match, since the effective detector "filter" is set by the CMOS detector response, much broader than the R-band filter. In addition, the satellite material reflectance properties change the input Solar spectrum into possibly something completely different, and therefore care should be taken on both accounts with the magnitude values listed in above in Table 2. All five labelled objects in Fig. 5 were comfortably detected in the median combined image, with SNRs exceeding 5.

The target tracking approach across a series of time-stepped images of resident space objects provides a few notable improvements over inertially (sidereal) tracked frames: 1) targets do not streak and stay within the field of view over a much longer time, 2) careful stacking of these target-tracked images co-adds target signal on the same detector pixels, and 3) median combined frames yield clean images almost completely devoid of stellar contamination. It is especially the latter that allows for sufficiently robust target tracking and photometry that can be executed on the spacecraft itself.

Conclusion

We successfully implemented an RSO tracking mode on a nanosatellite. The flight data collection campaign obtained sample RSO tracking data for targets spanning orbits in GEO, MEO, and LEO. A modified image processing approach mitigated challenges associated with datasets where stars are streaking across the image. We compared sensitivity versus standard inertial mode collects and observed an SNR improvement consistent with the number of frames averaged. We obtained additional improvements by averaging out residual warm pixels present in the image sets. We anticipate that future work will explore tracking at higher slew rates and extending this tracking technique to non-orbital space objects.